Original Article นิพนธ์ต้นฉบับ

การดำเนินโรคและการเปลี่ยนแปลงชั่วคราวที่พบในภาพรังสีทรวงอก ของผู้ป่วยติดเชื้อโควิด 19 ที่โรงพยาบาลพะเยา

วริสรา กิตติวรพงษ์กิจ พ.บ.
นายแพทย์ชำนาญการ (ด้านเวชกรรม) กลุ่มงานรังสีวิทยา โรงพยาบาลพะเยา

ส่งบทความ : 31 พ.ค. 2564
แก้ไขบทความ : 21 มิ.ย. 2564
ตีพิมพ์บทความ : 22 มิ.ย. 2564

บทคัดย่อ

ความเป็นมาและวัตถุประสงค์: การระบาดของโรคติดต่ออุบัติใหม่ คือโรค coronavirus disease 2019 (COVID -19) ในผู้ป่วยโรคนี้มีโอกาสที่จะเกิดภาวะปอดอักเสบ (pneumonia) ได้ สำหรับในประเทศไทย การตรวจภาพรังสีทรวงอกด้วยเครื่องเอกซเรย์เคลื่อนที่ (portable X-ray) เป็นการตรวจหลักในการวินิจฉัยและติดตามภาวะปอดอักเสบของผู้ป่วย COVID-19 การศึกษานี้จึงมีวัตถุประสงค์เพื่อศึกษาลักษณะภาพรังสีทรวงอกและติดตามการเปลี่ยนแปลงของภาพรังสีทรวงอก (chest X-ray) ในผู้ป่วย COVID-19 ที่ได้รับการถ่ายภาพด้วยเครื่อง portable X-ray ตลอดการเข้ารับการรักษาในโรงพยาบาล

รูปแบบการศึกษา: Retrospective descriptive study เก็บข้อมูลและวิเคราะห์ภาพถ่ายรังสีทรวงอก (chest X-ray) โดยมีการให้คะแนนตามระดับความรุนแรงของรอยโรคในปอดในผู้ป่วยติดเชื้อ COVID-19 ที่เข้ารับการรักษาในโรงพยาบาลพะเยาตั้งแต่วันที่ 10 เมษายน 2564 ถึง 15 พฤษภาคม 2564

ผลการศึกษา: ผู้ป่วยติดเชื้อ COVID-19 จำนวน 58 ราย (ชาย 30 ราย;51.7% หญิง 28 ราย;48.3%) อายุระหว่าง 2-79 ปี (ค่าเฉลี่ย 35.52 ± 16.80 ปี) มีความผิดปกติของภาพถ่ายรังสีทรวงอก (chest X-ray) 31 ราย (53.4%) จำนวนภาพถ่ายรังสีทรวงอก (chest X-ray) ผิดปกติที่นำมาวิเคราะห์จำนวน 172 รูปจากทั้งหมด 241 รูป (71.2%) ความผิดปกติทางรังสีที่พบมากที่สุดคือความผิดปกติชนิดเห็นเป็นปื้นๆ (ground glass opacities) กระจายในส่วนรอบนอกของปอดส่วนล่างทั้งสองข้าง ความผิดปกติชนิดนี้สามารถพัฒนาเป็นแบบหนาทึบ (consolidations) ที่กระจายในปอดสองข้างทั้งส่วนกลางและส่วนล่างได้ในช่วงสัปดาห์แรกหลังจากเข้ารับการรักษาในโรงพยาบาล โดยพบความผิดปกติทางรังสีรุนแรงที่สุดประมาณวันที่ 4-7 จากนั้นความผิดปกติจะลดลงและเริ่มพบความผิดปกติแบบร่างแห (reticulations) ประมาณวันที่ 9 หลังจากเข้ารับการรักษาในโรงพยาบาล แสดงถึงการเริ่มฟื้นฟูของโรค

สรุป: ภาพถ่ายรังสีทรวงอก (chest X-ray) ของผู้ป่วยมีการเปลี่ยนแปลงที่สามารถจำแนกเป็นกลุ่มตามความรุนแรงได้ ซึ่งเป็นประโยชน์ต่อการช่วยวินิจฉัย, ติดตามและพยากรณ์ความรุนแรงของโรคในผู้ป่วย COVID-19 ได้

คำสำคัญ: COVID-19 patients, COVID-19, chest X-ray, CXR

ติดต่อบทความ
วริสรา กิตติวรพงษ์กิจ กลุ่มงานรังสีวิทยา โรงพยาบาลพะเยา
Email: bow_wk@hotmail.com

Disease course and temporal changes of chest X-ray findings in COVID-19 positive patients at Phayao hospital

Warissara Kiththiworaphongkich MD.
Radiology department of Phayao hospital.

Submitted: 31 May 2021
Revised: 21 Jun 2021
Published: 22 Jun 2021

Background & Purpose: Since the outbreak of coronavirus disease 2019 (COVID-19) infection is progressing and worsening in various parts of the world. COVID-19 infection usually manifests clinically as pneumonia. In Thailand, portable chest X-ray (CXR) was the most commonly used modality for identification and follow up of lung abnormalities in COVID-19 positive patients. This study aims to describe the CXR findings and temporal radiographic changes in patients with confirmed COVID-19 throughout the admission period.

Material and Methods: A retrospective descriptive study of a laboratory confirmed COVID-19 patients by using RT-PCR who were admitted in Phayao hospital from April 10, 2021 to May 15, 2021. Patients' demographics, baseline CXR and serial follow up CXR were reviewed. A severity index was determined for each lung image. The lung finding scores were summed to produce the total severity score (TTS).

Results: A total of 58 patients (30 (51.7%) males and 28 (48.3%) females). Age of the patients ranged from 2 to 79 years old with mean age was 35.52 ± 16.80 years. A total of 241 chest x-rays were obtained for the 58 patients. Thirty-one in 58 patients (53.4%) had abnormal CXR findings at certain points of the disease course. There were 172 baseline CXR and serial CXR of 31 patients with abnormalities were analyzed to see temporal lung change. The most common finding on CXR was peripheral ground glass opacities (GGO) affecting the lower lung lobes. In the course of illness, the GGO progressed to diffuse consolidations affecting the middle and lower lung lobes around 1-8 days with peaking at day 1-4 after initial CXR. The severity of findings at CXR peaked at 4-7 days from initial CXR. The consolidations regressed and reticulations were developed over day 9 from initial CXR, indicating a healing phase. Bilateral middle lung zones and bilateral lower lung zones were the last areas of recovered.

Conclusion: This study showed that CXR was a good monitoring of COVID-19 radiologic manifestations and its scoring system provided a good method to predict the disease severity.

Keywords: COVID-19 patients, COVID-19, chest X-ray, CXR

Contact:
Warissara Kiththiworaphongkich, Radiology department of Phayao hospital.
Email: bow_wk@hotmail.com

INTRODUCTION

Since the beginning of the outbreak in December 2019 and labeling as a pandemic by the world health organization on March 11, 2020,[1] the global pandemic of coronavirus disease 2019 (COVID-19) infection is progressing and worsening in various parts of the world. At the time of writing (May 22, 2021), there are more than 166 million confirmed COVID-19 cases and nearly 3.5 million deaths in over 200 countries around the world. The numbers of cases still increased with no specific treatment , creating havoc for the health and financial systems of the world.[2]

In Thailand, reported the earliest case in January 2020.[3] COVID-19 has infected over 100,000 cases and continue to grow rapidly. COVID-19 infection caused by the novel coronavirus severe acute respiratory syndrome coronavirus 2 (SARS-CoV2) has been confirmed in many countries by real-time reverse transcription polymerase chain reaction (RT-PCR) on nasopharyngeal and throat swabs, with a positive rate of 30-70%.[4,5] Because of the primary involvement of the respiratory system, chest imagings are recommended in suspected COVID-19 cases for both evaluation and follow up. Computed tomography (CT) scan of the chest is more sensitive than chest X-rays (CXR) in terms of diagnosis and disease follow up,[6-7] but it is not feasible to use it as a preferred investigation due to infection control issues and lack of availability. In Thailand and many countries, portable CXR was the most commonly used modality for identification and follow up of lung abnormalities, also taking into account that CXR can be performed with portable equipment in isolation rooms. Such option also minimizes potential contact between patients and operators. The American College of Radiology notes that the CT decontamination required after scanning patients with COVID-19 may disrupt radiologic service availability and suggests that portable CXR may be considered to minimize the risk of cross infection.[8] However, images from portable machines produce a poorer quality image when compared with a CXR done in a dedicated radiography facility, therefore can be more difficult to interpret.[9]

For better assessment of the portable CXR findings of COVID-19, this study aims to describe the CXR findings and temporal radiographic changes in patients with confirmed COVID-19 throughout the admission period. Furthermore, this study will enhance radiologists and clinicians understanding of portable CXR findings in COVID-19. The hypothesis of this study is utilization of portable CXR for diagnosis and follow up of COVID-19 patient will help in early detection of progression to severe pneumonia in areas with limited access to chest CT.

MATERIALS AND METHOD

Study design

A retrospective descriptive study of a laboratory confirmed COVID-19 patients who were admitted to the isolation wards in Phayao hospital from April 10, 2021 to May 15, 2021. COVID-19 infection was confirmed by RT-PCR testing on nasopharyngeal swabs. All patients underwent portable CXR at admission and follow up portable CXR was performed in all but seven patients (seven in 58 patients had only baseline CXR). All CXR of COVID-19 confirmed patients were included in this study. A case record form was used to extract the data from the electronic medical records. Data collected included demographic characteristics and CXR findings.

The study was approved by the institutional Review Board of Phayao hospital (Reference number: 64-02-012).

Image acquisition and analyses

All the CXR were obtained as digital radiograph in the posteroanterior or anteroposterior projection using portable x-ray units for the isolation wards following the usual local protocols. Thirteen of CXR from other hospital before referring to Phayao hospital were also included. Three of the initial CXR was anteroposterior (3 of 58; 5%) and the rest was posteroanterior. Twenty-five of the follow-up CXR was anteroposterior (25 of 158; 15%) and the rest was posteroanterior. The CXR were analyzed by two radiologists who were blind to the symptoms followed by consensus.

Radiographic features including consolidation, ground-glass opacities (GGO) and reticulation were diagnosed according to the Fleischner society glossary of term.[10] Manifestations of pleural effusion or nodular opacity were also recorded.

Distribution of the lung lesions was categorized into 1) Peripheral predominance, perihilar predominance or diffuse. Peripheral and perihilar demarcation was defined as halfway between lateral edge of the lung and hilum). 2) right lung, left lung or bilateral. 3) Zonal distribution; upper zone, middle zone and lower zone. A severity score was determined for each lung using the Radiographic Assessment of Lung Edema (RALE) score.[11] The score is determined by the involvement of each lung by consolidations or GGO from 0 to 4 9 (0 = no involvement; 1 = < 25%; 2 = 25–50%; 3 = 50–75%; 4 = > 75% involvement). The scores for each lung were summed to produce the final severity score.Patients undergoing serial CXR were evaluated for the course of the disease. Baseline and serial CXR were reviewed and were compared to determine if there were progression, stability, or improvement of lung changes over the time course of the illness. The serial of follow up CXR

were categorized according to the time of the initial CXR; CXR performed at baseline (initial CXR), 1–4 days, 5–8 days, 9–12 days and over 13 days from initial CXR (day 0).

Data analysis

Quantitative variable like age is presented as mean along with age range. Qualitative variables including gender and clinical outcomes were presented as frequency and percentages. Outcome variable, portable CXR findings were presented as frequency and percentages.

RESULT

Patient's characteristics

A total of 58 confirmed COVID-19 patients (by RT-PCR from nasopharyngeal swabs) were admitted to the hospital during the study period. There were 30 (51.7%) males and 28 (48.3%) females. Age of the patients ranged from 2 to 79 years old with mean age was 35.52 ± 16.80 years. Table 1 shows patient's demographics characteristics and clinical outcomes.

Table 1 Patient's demographics characteristics and clinical outcomes (*n*=58)

Parameter	Number of Patients (%)
Sex	
Male	30 (51.7)
Female	28 (48.3)
Age (years), mean ± SD	35.52 ± 16.80
Clinical outcome at the end of the study	
Discharge	53 (91.4)
In admission	5 (8.6)
Died	0 (0)

Chest X-rays features

A total of 241 CXR were performed for 58 patients; 58 CXR at baseline and 183 CXR as follow up. Baseline CXR were performed for all patients at the day of admission. Baseline CXR was normal in 36 patients (62.1%), while 18 patients (31.0%) and 4 patients (6.9%) had abnormal baseline CXR and indeterminate CXR, respectively. During follow up CXR studies, 9 patients (15.5%) of the normal baseline CXR as well as all patients (4; 6.9%) in the indeterminate group showed CXR abnormalities. So CXR abnormalities were detected in 31 of 58 patients (53.4%) at certain points of the disease course (Table 2). Twenty-seven in 58 patients who tested positive for COVID-19 had negative CXR throughout their admission

Table 2 Distributions of baseline chest radiography (*n*=58)

Characteristic	No. of Patients (%)
No. of normal baseline CXR	36 (62.1)
No. of abnormal baseline CXR	18 (31.0)
No. of indeterminate baseline CXR	4 (6.9)
No. of patients with normal baseline CXR later becoming abnormal	9 (15.5)
No. of patients with indeterminate baseline CXR later becoming abnormal	4 (6.9)

At baseline CXR (Table 3), ground-glass opacities (GGO) were the most common findings (13 of 18; 72.2%), followed by consolidations (5 of 18; 27.8%). Peripheral distribution (14 of 18; 77.8%), lower zone distribution (13 of 18; 72.2%) and bilateral involvement (9 of 18; 50%) were more common in locations and distributions. 13 patients (72.2%) had mild radiographic findings with total severity score of 1-2. More extensive involvement was observed in 4 (22.2%) and 1 (5.6%) patients, who had severity scores of 3-4 and 7, respectively.

Table 3 Radiographic findings and distribution on baseline (initial) CXR in 18 patients

Parameter, n=18	Number of Patients (%)
Ground-glass opacities (GGO)	13 (66.7)
Consolidations	5 (27.8)
Distribution on CXR	
Peripheral predominant	14 (77.8)
Perihilar predominant	1 (5.6)
Diffuse	3 (16.7)
Right lung	5 (27.8)
Left lung	4 (22.2)
Bilateral lungs	9 (50)
Lobar involvement	
Right upper lung zone	1 (5.6)
Right middle lung zone	5 (27.8)
Right lower lung zone	12 (66.7)
Left upper lung zone	0
Left middle lung zone	0
Left lower lung zone	13 (72.2)

Baseline CXR and serial CXR of 31 patients with abnormalities at certain points of the disease course (172 CXR; baseline CXR = 31 and serial CXR = 141) were performed and analyzed to see the course of the disease and temporal lung change. The baseline (initial) CXR at was recorded as day 0, the frequency of findings was as follow; GGO = 13/31 (41.9%), consolidations = 5/31 (16.1%), normal 9/31 (29.1%) and indeterminate 4/31 (12.9%). On serial follow up CXR, GGO remained the most common lung abnormality pattern. At day 1-4 day from initial CXR, the frequency of the GGO was 23/50 (46%) and consolidations was 21/50 (42%). Two (4%) CXR were coarse reticulations and 4 (8%) CXR were normal. One patient with normal initial CXR (day 0), developed peribronchovascular consolidation in the LT lower lung zone (retrocardiac region) at day 3. One patient developed pleural effusion. The highest total chest radiography severity score (TTS) recorded was 8 at day 4.

At day 5-8, the frequency of CXR with GGO and consolidations decreased to 5/46 (10.9%) and 11/46 (23.9%) respectively. There were increased in the number of mixed patterns; GGO+nodular and consolidations+reticulations (21/46; 45.7%) and reticulations in 5/46; 10.9%. The rest of CXR (4/46; 8.7%) were normal. The highest TSS recorded was 8 at day 5-7.

At day 9-12, the GGO and consolidations regressed (1/28; 3.6% and 0, respectively) but increased frequency of mixed pattern of a nodular consolidations, GGO and reticulations (16/28; 57.1%). Reticulations and normal CXR were also increase in frequencies in this phase comprising 5/28;17.9% and 6/28;21.4% of the CXR, respectively. The highest TSS recorded was 6.

After day 13, the number of consolidation was zero (0). The GGO and the mixed pattern regressed, recorded in each 1 patient (1/17; 5.9%). There were increase in the number and frequency of the reticulations (11/17; 64.7%). The normal CXR was 4/17; 23.5% in this group. The highest TSS recorded was 4. Figure 1 shows the distribution of CXR findings at different time intervals from initial CXR.

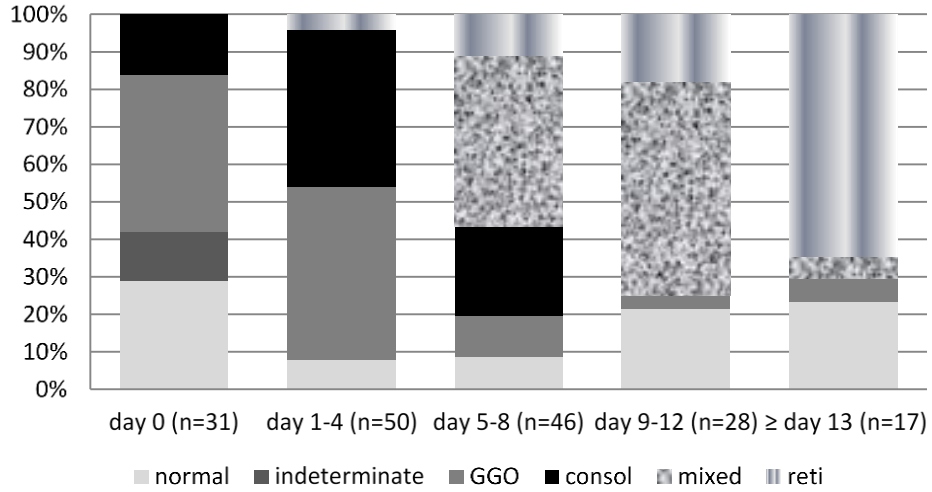

Figure 1 Temporal lung change of CXR findings.

Stacked-bar graph showed the distribution of lung findings on CXR at various time points from initial CXR. GGO was the most frequent abnormality on initial CXR, consolidations presented tilled the first week then was absent on subsequent CXR. Reticulations as well as mixed pattern of GGO, nodular consolidation and reticulations were gradually progressed in the second week. Normal CXR increased in frequency with time as patients showed radiological improvement. GGO = ground-glass opacity.

The spatial distribution of the radiographic lung changes were change throughout the course of the disease during admission. Earlier in the disease (baseline/initial CXR) the lung abnormalities were seen predominately in the periphery of the lungs, 14/31 (45.2%). Bilateral involvement was seen in 9/31 (29%). Unilateral involvement was seen in 5/31 (16.1%) on the right and 4/31 (13%) on the left. The lower zones were more frequency involved (32.2% right and 32.2% left).

At day 1-4 from initial CXR, the lung abnormalities extended from the periphery to the central giving much increase a diffuse pattern, from 9.7% (baseline CXR) to 44%. Bilateral involvement and lower zones involvement were noted in the majority of CXR. The numbers and percentage of the lower zones involvement and bilateral involvement were much increase (78% right lower zone ,78% left lower zone and 70% bilateral). The middle zones were more frequently involved (12.9% to 64% right and 6.5% to 42% left). Newly seen mild involvement of left upper zone was noted, 4%.

At day 5-8 from initial CXR, involvement of lower zones predominated (84.8% right and 78.3% left). Bilateral involvement and diffuse pattern were most common in this

stage (76.1% and 54.3%). Increase frequency of left upper zone involvement was seen, from 4% to 8.7%.

At day 9-12 from initial CXR, bilateral lower zones were predominated (64.2% and 71.4%, respectively), reflecting slow to recover. The frequency of RT middle zone and LT middle zone were 50% and 46.4%, respectively. Diffuse pattern were still predominant. Decrease frequency of right upper zone involvement were seen; from 10.9% to 3.6%. Complete resolution of left upper lung zone was noted.

After 13 days from initial CXR, bilateral middle zones, bilateral lower zones and isolated RT lung disease were the last to recover (70.6% RT middle, 76.5% RT lower, 58.8% left middle and 70.6% left lower). Complete resolution of perihilar lesion, isolated LT lung disease and bilateral upper zones involvement were seen. Bilateral upper zones were the least to be involved throughout the course of the illness. Few patients had exclusive involvement of central/perihilar of the lung with complete resolution. The frequency of normal CXR decreased from 29.1% at initial CXR to 8% at 1-4 days and 8.7% at 5-8 days, then increased to 21.4% at 9-12 days and 23.5% after 13 days. These represented the recovery periods. The specific frequencies of the spatial distribution of the temporal lung changes are in Figure 2.

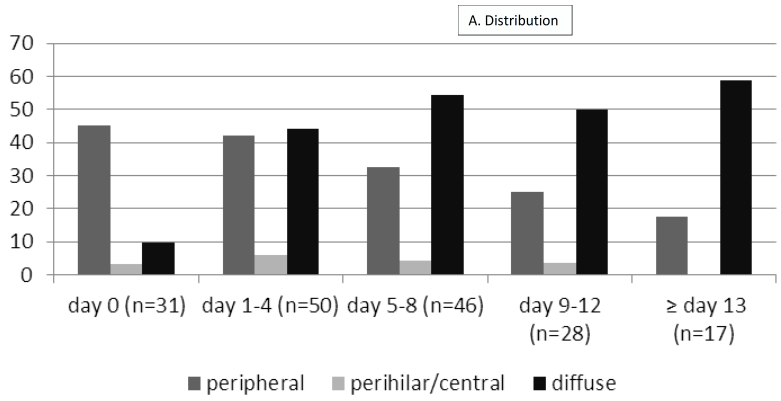

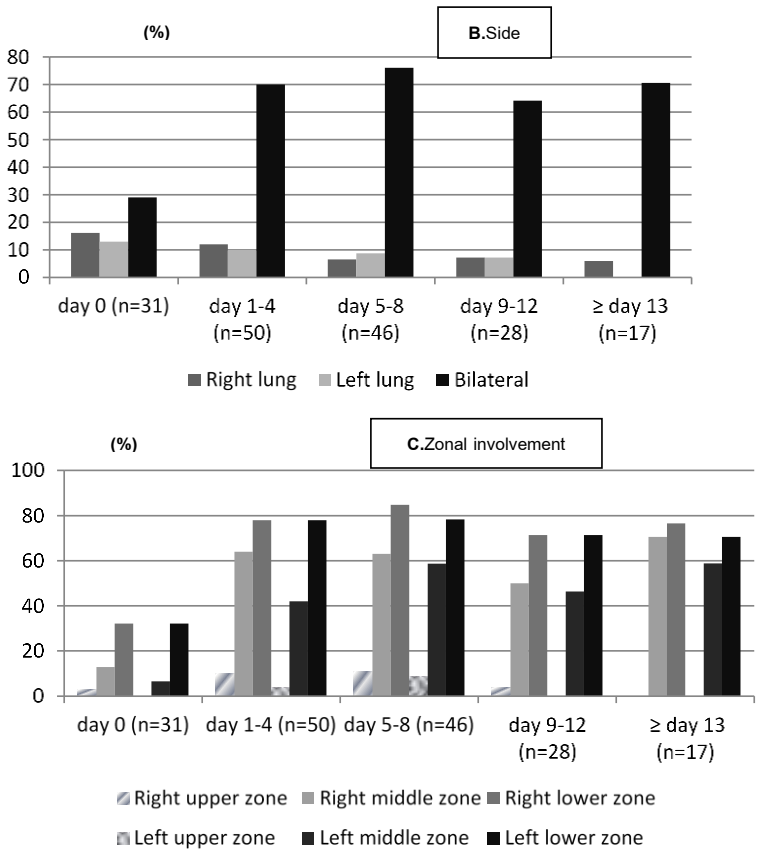

Figure 2 The spatial distribution of the lung changes at various time intervals from symptom onset. The lung changes were more frequently seen in a peripheral distribution on baseline/initial CXR, then developed to diffuse pattern on serial CXR. Bilateral distribution was more common than unilateral involvement. Bilateral lower lung zones remained the most frequently involved over time, but the upper zones were the least to be involved.

The details of disease course and temporal lung changes throughout the study period in 31 patients who had radiographic abnormalities on CXR are as described; One patient of indeterminate group progressed rapidly over an average period of 4 days seen as consolidations with increase TSS from 2 (day 1 from initial CXR) to 7 (day 3) and 8 (day 4). This patient showed gradual improvement from day 9-14 with regression of consolidations into GGO as well as development of reticulations at bilateral middle and lower lung zones, which remained stable until day 18 (the end of the study) Figure 3.

One patients of indeterminate group developed moderate findings on day 4 (TSS =4), which showed partial improvement on serial follow up CXR in day 5 (TTS = 3). Two patient of

indeterminate group developed mild findings (TTS = 1-2) with complete resolution in day 3 and day 9, respectively. At the end of the study, complete resolution was seen in 10 out of 31 patients who had initially mild disease (TTS = 1-2); 1 patient seen complete resolution at day 4, 2 patients in day 6-8, 4 patients in day 9-12 and 3 patients seen complete resolution over day 13. Figure 4. Only 1 patient who had initially severe disease with diffusely bilateral consolidations (TTS = 7) showed gradual improvement on serial day 6 CXR with regressed consolidations and increase reticulations and GGO (TSS at day 6 and day 11;last film = 4). One patient who had initial chest radiography severity score =4 with GGO showed developed consolidations in serial day 1-4 CXR with same chest radiography severity score then developed reticulations and GGO in day 8 (TTS, decrease from 4 to 2). One patient who had initial TSS =2 with consolidations showed decrease consolidation but developed reticulations on day 2 as well as residual reticulations on day 6 and 10 (TTS, decrease from 2 to 1). Two patients who had initial TTS =3-4 with consolidations and GGO showed developed reticulations and GGO in day 2 serial CXR with same chest radiography severity score, 1 patient had gradual improvement on day 6 serial CXR (TSS = 2) and 1 patient had stable CXR until day 4 (last film). Three patients who had initially mild disease (small GGO and normal baseline CXR) showed radiological worsening on serial CXR day 1-4 and day 5-8 (the highest TSS were 6-8) then gradual improvement in day 9-12 (the highest TSS were 4-6) and interval static after day 13 until the end of the study.

One patient who had initially mild disease (bilateral peripheral GGO, TSS = 2) progressed consolidations on day 2 (TSS = 4) then worsening on the daily serial CXR, the highest TSS = 6 at day 5. The abnormalities regressed as GGO, reticulations and decrease lung volume on day 9 (TSS = 3). These findings were interval static in day 9-12. Two patients who had initially mild disease (GGO, TSS = 1-2) progressed consolidations in day 5-8 (highest TSS = 5) then regressed as GGO and reticulations in day 9-12 (TSS = 2-3). Figure 5. One patient who had initially mild disease (GGO, TSS = 2) developed reticulations in day 5-8 with stable of TSS. Three patients with normal baseline CXR developed abnormality on serial CXR, as follows; 1 patient developed GGO on day 3 (TSS = 2), progressed to consolidations on day 6 (TSS = 3) and developed reticulations on day 10 (TSS = 2). Another 2 patients developed GGO in day 5-8 serial CXR (TSS = 3-4) then regressed to reticulations in day 9-12 without complete resolution. One patient with normal baseline CXR developed reticulations and a few tiny nodular

opacities at peripheral right lower lung zone (TSS = 1) on day 6 and day 10 CXR. One patient who had mild disease (RT peripheral GGO, TSS = 1) on baseline CXR without follow up serial CXR. The highest TSS recorded was 8 (the maximum possible score = 8). Peak severity score was reached at day 4-7 from initial CXR, represented the peak phase at which median TSS was 3. There were 7 out of 31 patients showed complete resolution of CXR abnormalities at over day 9 from initial CXR, could be the absorption phase.

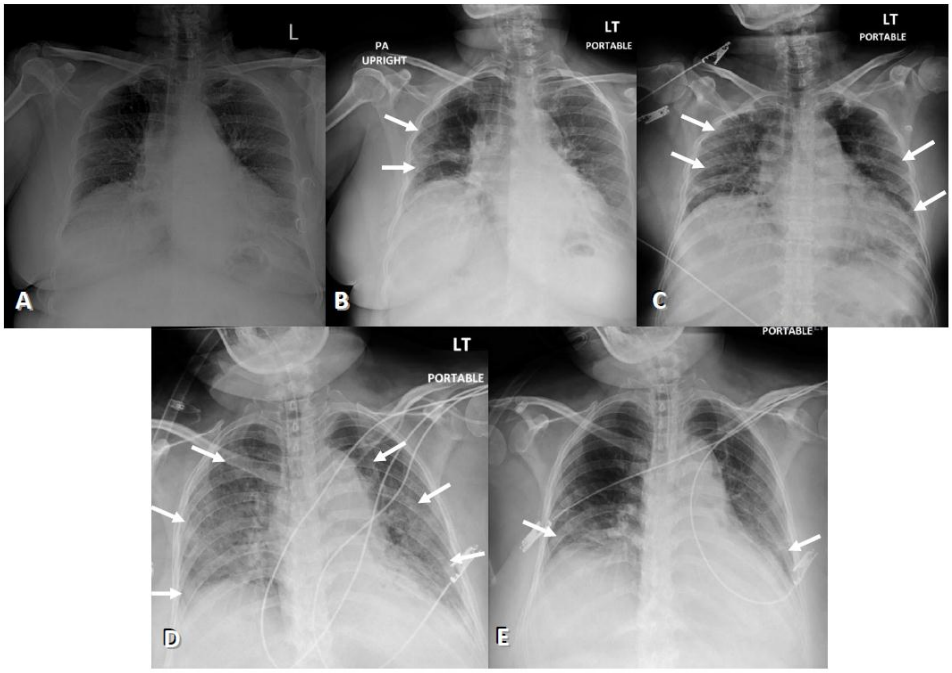

Figure 3 Series CXR in a 65-year-old woman with positive COVID-19 virus.
(A) initial CXR showed subtle poorly defined opacities at LT lower lung zone, indistinguishable between early/mild COVID-19 pneumonia or pseudolesion.
(B) CXR obtained on day 1 showed peripheral GGO and consolidations at right middle and lower lungzones (TSS =2, right 2 and left 0)
(C) CXR obtained on day 3 showed diffuse consolidations extended to all lung zones except for left upper zone (TSS =7, right 4 and left 3)
(D) CXR obtained on day 4 showed peaking of the findings with extensive diffuse patchy and nodular consolidations bilaterally (TSS =8, right 4 and left 4). The patient was intubated.
(E) CXR obtained on day 9 showed decrease degree of lung involvement with reduction of overall TSS. There were regression of consolidations into GGO as well as development of reticulations at middle and lower zones, bilaterally (TSS = 5, right 2 and left 3).

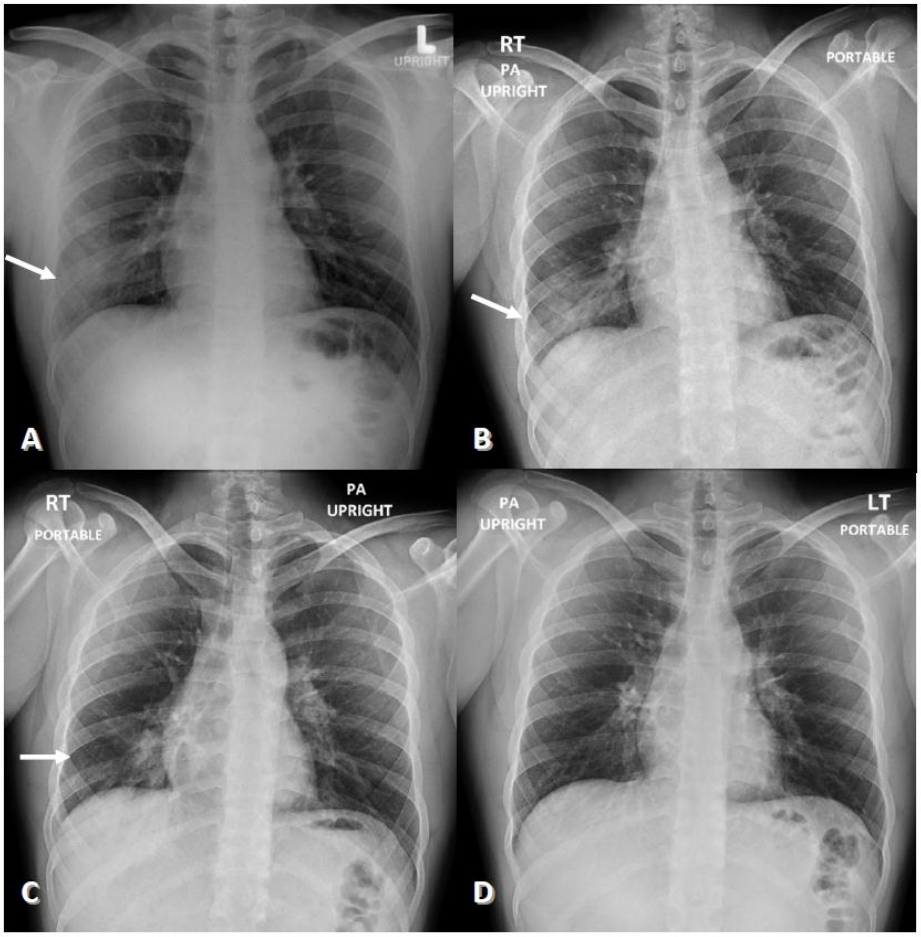

Figure 4 Series CXR in a 25-year-old man with positive COVID-19 virus.
(A) initial CXR showed peripheral right lower zonal consolidations with TSS = 1.
(B) CXR obtained on day 1 showed increase extension of right lower zonal consolidations involving both perihilar and periphery of the lung (TSS =2, right 2 and left 0).
(C) CXR obtained on day 3 showed regression of right lower zonal consolidations with development of reticulations at medial aspect (central) of right lower zone (TSS = 1, right 1 and left 0).
(D) CXR obtained on day 8 showed complete resolution of right lower zonal opacities.

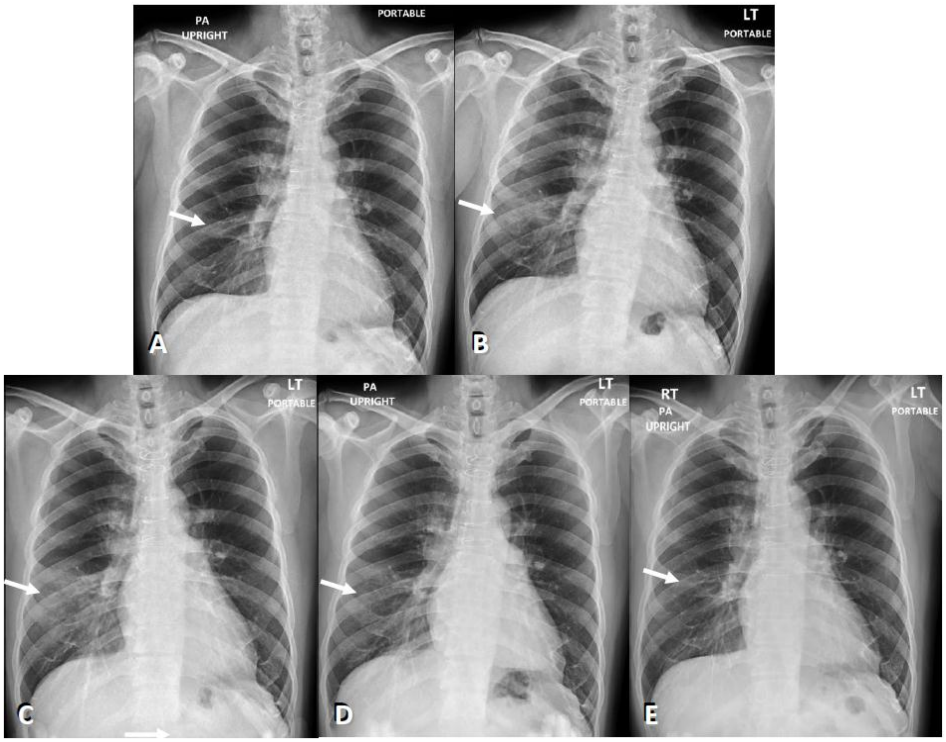

Figure 5 Series CXR in a 60-year-old man with positive COVID-19 virus.
(A) initial CXR showed small peripheral right lower zonal GGO with TSS = 1.
(B) CXR obtained on day 2 showed increase peripheral GGO at right lower zone (TSS =2, right 2 and left 0).
(C) CXR obtained on day 6 showed peaking of the findings with diffuse patchy consolidations mixed with GGO at right lower zone (TSS =2, right 2 and left 0).
(D) CXR obtained on day 9 showed regression of consolidations into GGO and development of reticulations at right lower zone (TSS = 2, right 2 and left 0).
(E) CXR obtained on day 13 showed complete resolution of GGO with residual reticulations at right lower zone, laterally to the RT hilum (TSS = 1, right 1 and left 0).

DISCUSSION

COVID-19 is a highly infectious disease that has been spread widely through the world. The management of disease primarily depends upon the early diagnosis.[12,13] Radiologic evaluation is one of the methods for diagnosis and follow up of COVID-19. Current literatures are mostly assessing COVID-19 chest CT findings, as it offers more sensitive results than CXR especially in initial assessment of the patients.[6-7] The high infectious rate of COVID-19 and the consequent increase in a radiologic examination would make the constant use of chest CT

scan (from diagnosis to discharge) difficult to sustain overtime.[14] This makes the CXR greatly substitute the CT examinations. The ACR has also recommended that portable CXR may be considered to minimized the risk of cross infection.[8] Although CXR is considered less sensitive for the detection of pulmonary involvement in early-stage disease , it is useful for assessing the course of COVID-19 disease and could be used as long term-term consequences monitoring.[15] To provide the valuable help for the physicians and improve the stratification of the disease risk, CXR scoring system was tailored providing a semi-quantitative tool for assessment of lung abnormalities.[7]

In this study, every patient had at least one portable CXR done during their admission period. No chest ct scan was performed in any of the patients. CXR abnormalities were detected in 31 of 58 patient (53.4%) proven to have COVID-19. The CXR abnormalities were analyzed for course of disease and temporal lung changes throughout their admission. The most common CXR findings in this study was GGO, followed by consolidations. These had peripheral distribution with bilateral lung involvement. There were lower lobes predilection of the opacities with the right lower lobe more common than the left lower lobe. These findings are in consensus with the previous studies on CXR and CT scans.[16-24] The diffuse consolidations as well as bilateral middle zones and lower zones involvements had progressed in 1 week after initial CXR (day 1-8), been peak at day 1-4 after initial CXR. Consolidations were both new lesions and transformation of GGO. The TTS had changed overtime, reached a peak at day 4-7 from initial CXR. One patient showed peribronchovascular consolidation, which were not common in the report of COVID-19 pneumonia.[25,26] One patient had pleural effusion during this phase, which was not common finding on chest imaging.[7,27] Phase of improvement of the CXR findings were seen in decreasing in size and extension of GGO/consolidations, regression of consolidation into GGO and reticulations which were seen over day 9 from initial CXR. Bilateral middle zones, bilateral lower zones and isolated RT lung disease were the last to recover.

The peak and the absorption (improvement) phases in this study were seen to be earlier than the previous studies in 2020 (peak phase range at days 5-15 and absorption phase range at days 10-17).[7,16,19,21,22] Four patients in determinate group were shortly repeated CXR on the next day. There was an article mentioned

about the features indistinguishable between equivocal/unsure/ indeterminate for COVID-19 pneumonia and other cause (e.g., pseudolesion), required clinical correlation and short-interval follow up CXR.[28]

The major strength of this study was the evaluation of serial CXR to see the temporal radiographic changes. This study had several limitations. First, it had a small sample size of 31 patients with abnormal CXR findings. Second, it was a retrospective study. Third, the lack of correlation between CXR severity score and clinical conditions of patients (such as onset of symptom, comorbidities, treatment). Fourth, not all the patients could be followed till the final outcome and lack of long term outcome. Fifth, the interval between serial CXR were not uniform as it was dedicated by clinicians as regards the clinical conditions, thus the affecting the precision of analysis. Sixth, for some severe case, the portable CXR (especially anteroposterior CXR) was suboptimal viewing, causing limited evaluation.

CONCLUSION

About 53.4% of patients with confirmed COVID-19 had abnormal CXR findings. The most common findings on CXR were GGO in a peripheral distribution with bilateral lower lobes predilection. The radiographic findings peaked at day 4-7 from initial CXR reaching the highest severity score and improved at over day 9 from initial CXR. The Radiographic Assessment of Lung Edema (RALE) score was used in this study with addition of bilateral middle zones involvement of COVID-19 as opposed to just lower zones involvement. As mentioned previously, portable CXR were the most readily available and feasible investigation in our set ups. This study showed that CXR from portable machine was a useful monitor of COVID-19 radiologic manifestations and its scoring system provided a good method to predict the disease severity. Therefore, radiologists and clinicians can all benefit from this study.

REFERENCES

1. World Health Organization. Novel coronavirus: China [Internet]. c2021 [cited 2021 May 1]. Available from: https://www.who.int/director-general/speeches/detail/who-director-general-s-opening-remarks-at-the-media-briefing-on-covid-19---11-march-2020
2. Sun P, Lu X, Xu C, Sun W, Pan B. Understanding of COVID–19 based on current evidence. J Med Virol. 2020;92(6):548-51. doi: 10.1002/jmv.25722.

3. Ratnarathon A. Coronavirus infectious disease-2019 (COVID-19): a case report, the first patient in Thailand and outside China. J Bamrasnaradura Infect Dis Inst. 2020;14(2):116-23.
4. Ai T, Yang Z, Hou H, Zhan C, Chen C, Lv W, et al. Correlation of chest CT and RT-PCR testing incoronavirus disease 2019 (COVID-19) in China: a report of 1014 cases. Radiology. 2020;296(2):E32-40. doi: 10.1148/radiol.2020200642.
5. Fang Y, Zhang H, Xie J, Lin M, Ying L, Pang P, et al. Sensitivity of chest CT for COVID-19: comparison to RT-PCR. Radiology. 2020;296(2):E115-7. doi: 10.1148/radiol.2020200432.
6. Ng MY, Lee EYP, Yang J, Yang F, Li X, Wang H, et al. Imaging profile of the COVID-19 infection: Radiologic findings and literature review. Radiol Cardiothorac Imaging. 2020;2(1):e200034. doi: https://doi.org/10.1148/ryct.2020200034.
7. Wong HYF, Lam HYS, Fong AHT, Leung ST, Chin TWY, Lo CSY, et al. Frequency and distribution of chest radiographic findings in COVID-19 positive patients. Radiology. 2020;296(2):E72–78. doi: 10.1148/radiol.2020201160.
8. American College of Radiology. ACR recommendations for the use of chest radiography and computed tomography (CT) for suspected COVID-19 infection [Internet]. c2020 [update 2020 March 11; cited 2021 May 1]. Available from: https://www.acr.org/Advocacy-and-Economics/ACR-Position-Statements/Recommendations-for-Chest-Radiography-and-CT-for-Suspected-COVID19-Infection
9. Cleverley J, Piper J, Jones MM. The role of chest radiography in confirming covid-19 pneumonia. BMJ. 2020;370:m2426. doi: 10.1136/bmj.m2426
10. Hansell DM, Bankier AA, MacMahon H, McLoud TC, Müller NL, Remy J. Fleischner Society: glossary of terms for thoracic imaging. Radiology. 2008;246(3):697-722. doi: 10.1148/radiol.2462070712.
11. Warren MA, Zhao Z, Koyama T, Bastarache JA, Shaver CM, Semler MW, et al. Severity scoring of lung oedema on the chest radiograph is associated with clinical outcomes in ARDS. Thorax. 2018;73(9):840–6.
12. Toussie D, Voutsinas N, Finkelstein M, Cedillo MA, Manna S, Maron SZ, et al. Clinical and Chest Radiography Features Determine Patient Outcomes in Young and Middle-aged Adults with COVID-19. Radiology. 2020;297(1):E197–206. doi: 10.1148/radiol.2020201754.
13. Chung M, Bernheim A, Mei X, Zhang N, Huang M, Zeng X, et al. CT imaging features of 2019 novel coronavirus (2019-nCoV). Radiology. 2020;295(1):202–7.

14. Borghesi A, Maroldi R. COVID-19 outbreak in Italy: experimental chest X-ray scoring system for quantifying and monitoring disease progression. Radiol Med. 2020;125(5):509-13. doi: 10.1007/s11547-020-01200-3.
15. Yasin R, Gouda W. Chest X-ray findings monitoring COVID-19 disease course and severity. Egypt J Radiol Nucl Med. 2020;51:193. doi: https://doi.org/10.1186/s43055-020-00296-x.
16. Rousan LA, Elobeid E, Karrar M, Khader Y. Chest x-ray findings and temporal lung changes in patients with COVID-19 pneumonia. BMC Pulm Med. 2020;20(1):245. doi: 10.1186/s12890-020-01286-5.
17. Ratnarathon A. Clinical characteristics and chest radiographic findings of coronavirus disease 2019 (COVID-19) pneumonia at Bamrasnaradura Infectious Disease Institute. Dis Control J. 2020;46(4):540-50.
18. Jacobi A, Chung M, Bernheim A, Eber C. Portable chest X-ray in coronavirus disease-19 (COVID-19): a pictorial review. Clin Imaging. 2020;64:35-42. doi: 10.1016/j.clinimag.2020.04.001.
19. Vancheri SG, Savietto G, Ballati F, Maggi A, Canino C, Bortolotto C, et al. Radiographic findings in 240 patients with COVID-19 pneumonia: time-dependence after the onset of symptoms. Eur Radiol. 2020;30(11):6161-9. doi: 10.1007/s00330-020-06967-7.
20. Chen N, Zhou M, Dong X, Qu J, Gong F, Han Y, et al. Epidemiological and clinical characteristics of 99 cases of 2019 novel coronavirus pneumonia in Wuhan, China: a descriptive study. Lancet. 2020;395(10223):507–13.
21. Wang Y, Dong C, Hu Y, Li C, Ren Q, Zhang X, et al. Temporal changes of CT findings in 90 patients with COVID-19 pneumonia: a longitudinal study. Radiology. 2020;296(2):E55-64. doi: 10.1148/radiol.2020200843.
22. Pan F, Ye T, Sun P, Gui S, Liang B, Li L, et al. Time course of lung changes on chest CT during recovery from 2019 novel coronavirus (COVID-19) pneumonia. Radiology. 2020;295(3):715–21. doi: 10.1148/radiol.2020200370.
23. Zhou S, Wang Y, Zhu T, Xia L. CT features of coronavirus disease 2019(COVID-19) pneumonia in 62 patients in Wuhan, China. AJR Am J Roentgenol. 2020;214(6):1287-94. doi: 10.2214/AJR.20.22975.
24. Durrani M, Haq IU, Kalsoom U, Yousaf A. Chest X-ray findings in COVID 19 patients at a University Teachinng Hospital - A descriptive study. Pak J Med Sci. 2020;36(COVID19-S4):S22-26. doi: 10.12669/pjms.36.COVID19-S4.2778.

25. Bernheim A, Mei X, Huang M, Yang Y, Fayad ZA, Zhang N, et al. Chest CT findings in coronavirus Disease-19 (COVID-19): relationship to duration of infection. Radiology. 2020;295(3):200463.
26. Piyavisetpat N, Pongpirul K, Sukkasem W, Pantongrag-Brown L. 'Ring of fire' appearance in COVID-19 pneumonia. BMJ Case Rep. 2020;13(6):e236167. doi: 10.1136/bcr-2020-236167.
27. Wu G, Li X. Moblie x-rays are highly valuable for critically ill COVID patients. Eur Radiol. 2020;30(9):5217–19. doi: 10.1007/s00330-020-06918-2.
28. ฐิติพร สุวัฒนะพงศ์เชฏ, ชญานิน นิติวรางกูร, วราวุฒิ สุขเกษม, สิทธิ์ พงษ์กิจการุณ. คู่มือเกณฑ์การคัดแยกระดับความผิดปกติจากภาพรังสีทรวงอกเพื่อใช้สำหรับการวินิจฉัยภาวะปอดอักเสบในผู้ป่วยโรคโควิด 19 (เวอร์ชัน 1). กรุงเทพฯ: ภาควิชารังสีวิทยา คณะแพทยศาสตร์โรงพยาบาลรามาธิบดี มหาวิทยาลัยมหิดล; 2564 [เข้าถึงเมื่อ 1 พฤษภาคม 2564]. เข้าถึงได้จาก: https://med.mahidol.ac.th/radiology/sites/default/files/public/knowledge/20210505050251.pdf